Longimicins A−D: Novel Bioactive Acetogenins from *Asimina longifolia* (Annonaceae) and Structure−Activity Relationships of Asimicin Type of Annonaceous Acetogenins

Qing Ye, Kan He, Nicholas H. Oberlies, Lu Zeng, Guoen Shi, Dean Evert,[†] and Jerry L. McLaughlin*

Department of Medicinal Chemistry and Pharmacognosy, School of Pharmacy and Pharmacal Sciences, Purdue University, West Lafayette, Indiana 47907, and Department of Horticulture, Georgia Agricultural Experimental Station, University of Georgia, Tifton, Georgia 31793

Received January 16, 1996[⊗]

Bioactivity-directed fractionation of the ethanol extract of *Asimina longifolia* led to the isolation of four novel bioactive annonaceous acetogenins: longimicins A−D (**1**−**4**). Compounds **1**−**4** represent the asimicin type of acetogenins; however, the locations of the adjacent bis-tetrahydrofuran (THF) ring moieties are shifted along the aliphatic chains compared to the known compounds of this type. They are the first examples among this type of acetogenins with the placements of the ring systems altered. Compounds **1**−**4** showed bioactivities in several bioassays, but they are less active than their structural isomers. Study of their structure−activity relationships (SAR) reveals that the position of the adjacent bis-THF ring moiety is essential for maximization of the bioactivities among these asimicin type annonaceous acetogenins.

Introduction

Annonaceous acetogenins are derivatives of C32 or C34 fatty acids. These compounds have terminal γ-lactone rings, zero to three tetrahydrofuran (THF) rings, and a number of oxygenated moieties in the middle of the long hydrocarbon chains.[1−3] Acetogenins can be categorized to certain "types" according to the number and arrangement of the THF rings, as well as the configuration of the stereogenic centers within and adjacent to the THF moieties.[3] The asimicin type of acetogenins[4] is characterized by the presence of an adjacent bis-THF ring with two flanking hydroxyls, and within the bis-THF ring system, the pseudosymmetrical *threo/trans/threo/trans/threo* pattern[5,6] of relative configuration is displayed. Some asimicin type compounds show highly potent antitumor and pesticidal activities,[1−4,7] suggesting promising future medicinal and agricultural applications for this group of compounds.

Activity-directed fractionation of the ethanol extract of the leaves and twigs of *Asimina longifolia* K. (Annonaceae), using the brine shrimp lethality test (BST) to monitor fractionation,[8,9] led to the isolation of four new asimicin type acetogenins, which were named longimicins A−D (**1**−**4**). Compounds **1**−**4** (Figure 1) all have the structural novelty that their THF ring systems are shifted by two or four carbon units along the hydrocarbon chains compared with the previously reported compounds of the asimicin type.[1−3] The determinations of the positions of the THF ring systems were based on the EIMS analyses of their tri-TMSi derivatives. The structures and stereochemistries were elucidated by analyses of 1D and 2D NMR spectra before and after certain chemical derivatizations. Several bioassays were carried out to test the bioactivities of compounds **1**−**4**, and comparison of their activities with those of the known compounds revealed the essential nature of the position of the THF ring moiety for maximizing the bioactivities of the asimicin type acetogenins.

Results and Discussion

Chemistry. Compound **1** was isolated as a colorless wax. The molecular weight of **1** was determined by a peak at *m/z* 623 [MH$^+$] in the FABMS. HRFABMS found the molecular ion peak at *m/z* 623.4880 which closely matched the exact mass, 623.4887, calculated for the molecular formula, $C_{37}H_{66}O_7$.

The spectral data of **1** showed an IR carbonyl absorption at 1750 cm^{-1}, a UV (MeOH) λ_{max} at 208 nm (log ϵ 3.80), proton resonances at δ 7.19 (H-35), 5.06 (H-36), 3.86 (H-4), 2.53 (H-3a), 2.40 (H-3b), and 1.41 (H-37) in the ^{1}H-NMR spectra, and carbon resonances at δ 174.5 (C-1), 151.8 (C-35), 131.1 (C-2), 78.0 (C-36), 70.1 (C-4), and 19.2 (C-37) in the ^{13}C-NMR spectra. These are all characteristic spectral features for the methylated α,β-unsaturated γ-lactone ring with a 4-OH moiety, as commonly found in the annonaceous acetogenins.[1−3]

The existence of three OH moieties in **1** was evidenced by a prominent IR OH absorption at 3400 cm^{-1}, three successive losses of H_2O (*m/z* 18) from the [MH$^+$] in the FABMS, and the preparation of tri-acetate (**1a**) and tri-TMSi (**1b**) derivatives. The presence of an adjacent bis-THF ring system with two flanking hydroxyls in **1** was indicated by the ^{1}H-NMR signals at δ 3.39 (H-11, H-20), 3.83 (H-12, H-15, H-16, and H-19), and ^{13}C signals at δ 74.1 (H-11, H-20), 83.2 (C-12, H-19), 81.8 (C-15, C-16) (Table 1). EIMS of **1b** (Figure 2) determined this moiety to be located at C-11−C-20. The placement was further confirmed by HREIMS of **1b**, in which the exact mass was determined for the fragment at *m/z* 399.2379 (calcd 399.2387) corresponding to the elemental composition of $C_{20}H_{39}O_4Si_2$.

The relative stereochemistry across the THF ring and the flanking hydroxyls was assigned as *threo/trans/threo/trans/threo* based on ^{1}H- and ^{13}C-NMR data of **1**

[†] University of Georgia.
[⊗] Abstract published in *Advance ACS Abstracts,* April 1, 1996.

0022-2623/96/1839-1790$12.00/0

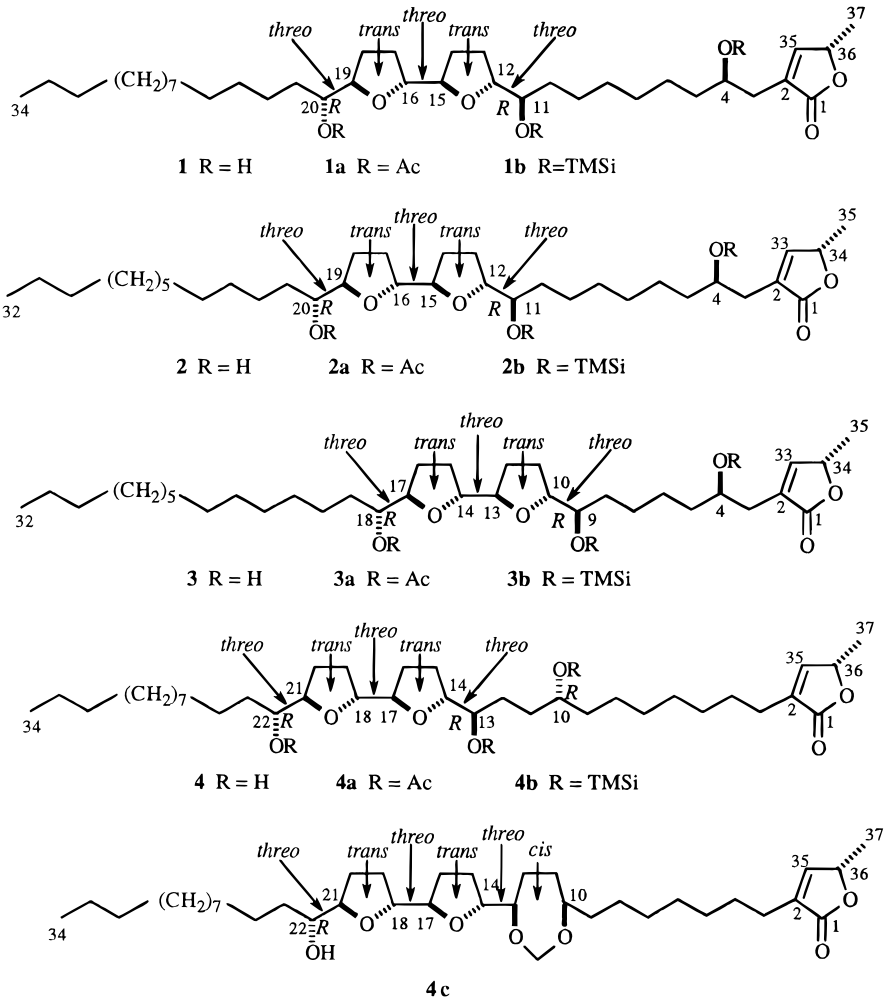

Figure 1. Chemical structures of **1**, **1a**,**b**, **2**, **2a**,**b**, **3**, **3a**,**b**, **4**, and **4a**–**c**.

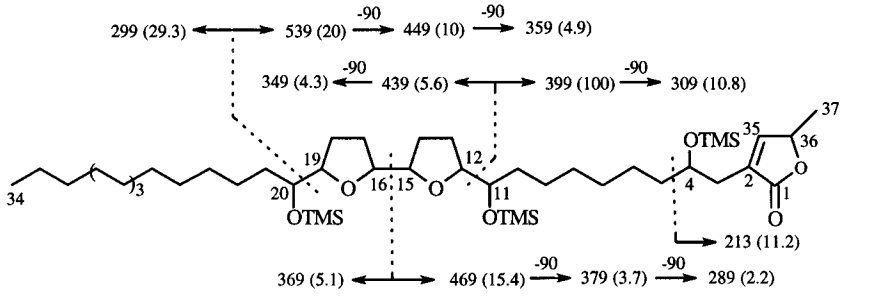

Figure 2. Diagnostic mass fragmentation ions of **1b** (molecular mass = 838 amu) in *m*/*z*, with percent intensities in parentheses. Losses of *m*/*z* 90 indicate the loss of TMSiOH neutrals.

and **1a**, which were consistent with those of model compounds.[5,6] The absolute stereochemistries were determined as C-4*R*, C-11*R*, and C-20*R* by using advanced Mosher ester methodology (Table 5).[10] Comparing the NMR data of the MTPA derivatives of **1** with those of model butenolides synthesized by Hoye *et al.*,[11] the relative stereochemistry between C-4 and C-36 was revealed as "unlike" (*RS* or *SR*). Thus, the absolute stereochemistry for C-36 was determined as *S*, as is usual for all the known acetogenins.

Therefore, the structure of **1** was concluded to be as illustrated and named longimicin A. Longimicin A is a structural isomer of asimicin,[4] the only difference between them is the location of the THF ring moiety which is shifted by four carbon units toward the γ-lactone ring in **1** compared with asimicin.

Compounds **2** and **3** (Table 2 and 3) were both isolated as colorless waxes. FABMS gave them the same molecular ion peak at *m*/*z* 595 [MH^+], and HRFABMS established the molecular formulas of both **2** and **3** to be $C_{35}H_{62}O_7$ by showing their [MH^+] peaks at *m*/*z* 595.4718 (**2**) and 595.4736 (**3**) (calcd 595.4754).

The IR, UV, and ^{1}H- and ^{13}C-NMR spectra of **2** and **3** were very similar to those of **1**. Comparisons of these spectra gave the indication that **2** and **3** might also possess the identical structural skeleton as that of **1**; this included the terminal α,β-unsaturated γ-lactone ring with a 4-OH group and an adjacent bis-THF ring with two flanking hydroxyls; however, **2** and **3** had chain lengths of C-35 instead of C-37. The relative configuration in the bis-THF ring moieties was also defined as *threo*/*trans*/*threo*/*trans*/*threo* based on the ^{1}H-NMR

Table 1. ^{1}H-NMR (500 MHz, $CDCl_3$) and ^{13}C-NMR (125.75 MHz, $CDCl_3$) Data for Longimicin A (**1**) and Its Triacetate Derivative (**1a**)

	δ_H (J, Hz)		δ_C
H/C no.	**1**	**1a**	**1**
1			174.52
2			131.15
3a	2.53 ddt (15.1, 3.2, 1.6)	2.56 ddt (15.1, 3.2, 1.6)	33.52
3b	2.40 ddt (15.1, 8.2, 1.3)	2.52 ddt (15.1, 8.2, 1.3)	
4	3.86 m	5.09 m	70.05
5−10	1.20−1.50 m	1.20−1.50 m	22.74−37.74
11	3.39 m	4.86 m	74.09
12	3.83 m	3.98 m	83.23
13a, 18a	1.98 m	1.98 m	22.74−37.74
13b, 18b	1.53−1.70 m	1.58 m	22.74−37.74
14a, 17a	1.98 m	1.92 m	22.74−37.74
14b, 17b	1.53−1.70 m	1.79 m	22.74−37.74
15	3.83 m	3.90 m	81.82
16	3.83 m	3.90 m	81.82
19	3.83 m	3.98 m	83.15
20	3.39 m	4.86 m	74.17
21−33	1.20−1.50 m	1.20−1.50 m	22.74−37.74
34	0.88 t (7.0)	0.88 t (7.0)	14.17
35	7.19 q (1.4)	7.19 q (1.4)	151.82
36	5.06 qq (6.8, 1.5)	5.01 qq (6.8, 1.5)	78.02
37	1.41 d (6.9)	1.41 d (6.9)	19.19
4-OAc		2.04 s	
11-OAc		2.08 s	
20-OAc		2.08 s	

Table 2. ^{1}H-NMR (500 MHz, $CDCl_3$) and ^{13}C-NMR (125.75 MHz, $CDCl_3$) Data for Longimicin B (**2**) and Its Triacetate Derivative (**2a**)

	δ_H (J, Hz)		δ_C
H/C no.	**2**	**2a**	**2**
1			174.52
2			131.15
3a	2.53 ddt (15.1, 3.2, 1.6)	2.56 ddt (15.1, 3.2, 1.6)	33.45
3b	2.40 ddt (15.1, 8.2, 1.3)	2.52 ddt (15.1, 8.2, 1.3)	
4	3.86 m	5.09 m	69.96
5−10	1.20−1.50 m	1.20−1.50 m	22.74−37.74
11	3.39 m	4.86 m	74.00
12	3.83 m	3.98 m	83.14
13a, 18a	1.98 m	1.98 m	22.74−37.74
13b, 18b	1.53−1.70 m	1.58 m	22.74−37.74
14a, 17a	1.98 m	1.92 m	22.74−37.74
14b, 17b	1.53−1.70 m	1.79 m	22.74−37.74
15	3.83 m	3.90 m	81.74
16	3.83 m	3.90 m	81.74
19	3.83 m	3.98 m	83.14
20	3.39 m	4.86 m	74.09
21−31	1.20−1.50 m	1.20−1.50 m	22.74−37.74
32	0.88 t (7.0)	0.88 t (7.0)	14.17
33	7.19 q (1.4)	7.19 q (1.4)	151.73
34	5.06 qq (6.8, 1.5)	5.01 qq (6.8, 1.5)	77.93
35	1.41 d (6.9)	1.41 d (6.9)	19.09
4-OAc		2.04 s	
11-OAc		2.08 s	
20-OAc		2.08 s	

spectral analyses of **2**, **2a**, **3**, and **3a**.[5,6] By using the advanced Mosher ester methodology[7] and Hoye's method (Table 5),[11] the absolute stereochemistries of the chiral centers in **2** and **3** were determined to be the same as those of **1**.

The placement of the adjacent bis-THF ring system was determined on the basis of the EIMS fragmentation pattern of the TMSi derivatives of **2** (**2b**) (Figure 3) and **3** (**3b**) (Figure 4). The ring system was determined to be located at C-11−C-20 for **2**, and at C-9−C-18 for **3**.

Table 3. ^{1}H-NMR (500 MHz, $CDCl_3$) and ^{13}C-NMR (125.75 MHz, $CDCl_3$) Data for Longimicin C (**3**) and Its Triacetate Derivative (**3a**)

	δ_H (J, Hz)		δ_C
H/C no.	**3**	**3a**	**3**
1			174.52
2			131.15
3a	2.53 ddt (15.1, 3.2, 1.6)	2.56 ddt (15.1, 3.2, 1.6)	33.37
3b	2.40 ddt (15.1, 8.2, 1.3)	2.52 ddt (15.1, 8.2, 1.3)	
4	3.86 m	5.09 m	69.75
5−8	1.20−1.50 m	1.20−1.50 m	22.74−37.74
9	3.39 m	4.86 m	73.82
10	3.83 m	3.98 m	83.16
11a, 16a	1.98 m	1.98 m	22.74−37.74
11b, 16b	1.53−1.70 m	1.58 m	22.74−37.74
12a, 15a	1.98 m	1.92 m	22.74−37.74
12b, 15b	1.53−1.70 m	1.79 m	22.74−37.74
13	3.83 m	3.90 m	81.76
14	3.83 m	3.90 m	81.76
17	3.83 m	3.98 m	83.00
18	3.39 m	4.86 m	74.09
19−31	1.20−1.50 m	1.20−1.50 m	22.74−37.74
32	0.88 t (7.0)	0.88 t (7.0)	14.17
33	7.19 q (1.4)	7.19 q (1.4)	151.82
34	5.06 qq (6.8, 1.5)	5.01 qq (6.8, 1.5)	77.94
35	1.41 d (6.9)	1.41 d (6.9)	19.19
4-OAc		2.04 s	
9-OAc		2.08 s	
18-OAc		2.08 s	

Compounds **2** and **3** were given the trivial names longimicins B and C, respectively. **2** and **3** are structural isomers of parviflorin,[12] and they differ from parviflorin only in that the position of the THF ring system is at C-13−C-22 in parviflorin. Thus, the ring system is shifted by two carbon units in **2** and four carbon units in **3** toward the γ-lactone ring.

Compound **4** was isolated as another waxy compound. A molecular ion peak at m/z 623 in the FABMS spectrum of **4** once again indicated a molecular weight of 622 as in **1** and asimicin. The HRFABMS spectrum showed an exact mass peak at m/z 623.4880, which matched the molecular formula $C_{37}H_{66}O_7$ (calcd 623.4887).

The NMR spectral data of **4** also provided the characteristic features for the α,β-unsaturated γ-lactone, but without the 4-OH group (Table 4). The absence of the 4-OH group is evidenced by the upfield shifts, compared with **1**−**3**, for three proton resonances at δ 6.99 (H-35), 5.00 (H-36), and 2.26 (H-3) and four carbon resonances at δ 174.0 (C-1), 148.8 (C-35), 134.3 (C-2), and 77.4 (C-36). H-3 in **1**−**3** gave two doublet doublet triplet signals at δ 2.53 and 2.40 due to the chiral center at C-4, while the signals in **4** were combined into one triplet triplet at δ 2.26, showing the absence of the 4-OH in **4**. Furthermore, the proton integration for the multiplet at δ 3.83−3.87 in **4** is one proton less than those of **1**−**3**, but there is one more proton resonance at δ 3.62, suggesting that the 4-OH group is absent in **4** and that another OH is present somewhere in the middle of the aliphatic chain.

As determined with compounds **1**−**3**, the presence of an adjacent bis-THF ring with two flanking hydroxyls was obvious from the ^{1}H- and ^{13}C-NMR spectra of **4**. A total of three OH groups were recognized by analyses of FABMS, IR, ^{1}H-NMR, and ^{13}C-NMR of **4** and its triacetate derivative (**4a**). The carbon skeleton of **4** was determined on the basis of the EIMS spectrum of its

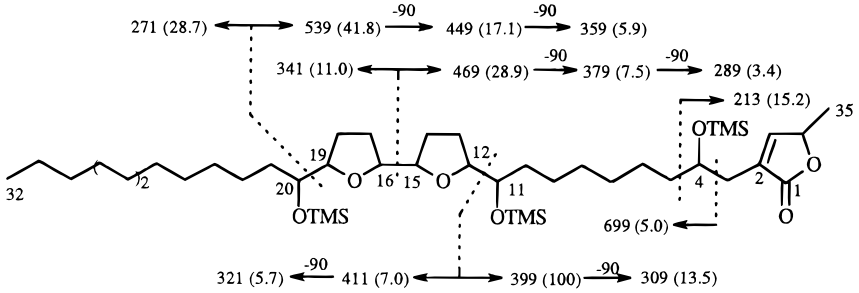

Figure 3. Diagnostic mass fragmentation mass ions of **2b** (molecular mass = 810 amu) in *m*/*z*, with percent intensities in parentheses. Losses of *m*/*z* 90 indicate the loss of TMSiOH neutrals.

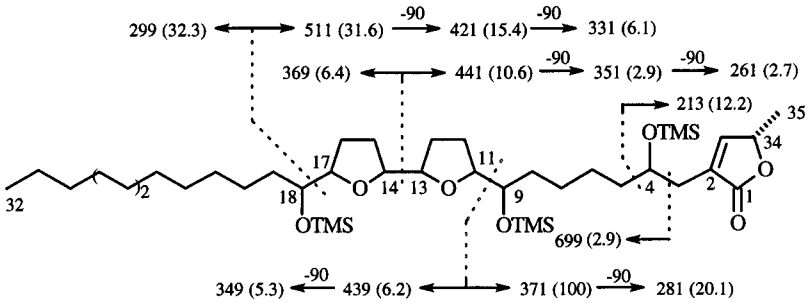

Figure 4. Diagnostic mass fragmentation ions of **3b** (molecular mass = 810 amu) in *m*/*z*, with percent intensities in parentheses. Losses of *m*/*z* 90 indicate the loss of TMSiOH neutrals.

Table 4. ^{1}H-NMR (500 MHz, $CDCl_3$) and ^{13}C-NMR (125.75 MHz, $CDCl_3$) Data for Longimicin D (**4**), Its Triacetate Derivative (**4a**), and Its Formaldehyde Acetal Derivative (**4c**)

	δ_H (J in Hz)			δ_C
H/C no.	**4**	**4a**	**4c**	**4**
1				173.91
2				134.33
3	2.26 tt (8.0, 1.5)	2.26 tt (8.0, 1.5)	2.26 tt (8.0, 1.5)	22.65−37.57
4−9	1.21−1.62 m	1.21−1.62 m	1.21−1.62 m	22.65−37.57
10	3.62 m	4.80−4.88 m	3.67 m	71.72
11, 12	1.21−1.62 m	1.21−1.62 m	1.53 m, 1.80 m	22.65−37.57
13	3.44 m	4.80−4.88 m	3.69 m	74.21
14	3.86 m	3.99 dt	4.04 dt (8.0, 6.0)	82.85
15a, 20a	1.98 m	1.96 m	1.96 m	22.65−37.57
15b, 20b	1.63 m	1.60 m	1.55−1.70 m	22.65−37.57
17, 18	3.86 m	3.90 m	3.95dt, 3.89 dt	81.69
16a, 19a	1.98 m	1.91 m	1.95 m	22.65−37.57
16b, 19b	1.63 m	1.78 m	1.69 m	22.65−37.57
21	3.86 m	3.99 dt	3.82 dt (8.0, 6.0)	83.15
22	3.39 m	4.80−4.88 m	3.38 m	74.06
23−33	1.21−1.62 m	1.21−1.62 m	1.21−1.62 m	22.65−37.57
34	0.878 t (7.0)	0.878 t (7.0)	0.878 t (7.0)	14.08
35	6.99 q (1.5)	6.99 q (1.5)	6.99 q (1.5)	148.8
36	4.99 qq (6.8, 1.5)	4.99 qq (6.8, 1.5)	4.99 qq (6.8, 1.5)	77.41
37	1.41 d (7.0)	1.41 d (7.0)	1.41 d (7.0)	19.19
10-OAc		2.04 s		
13-OAc		2.08 s		
22-OAc		2.07 s		

Table 5. ^{1}H-NMR (500 MHz, $CDCl_3$) Data for MTPA Derivatives of Compounds **1**−**3**

H no.	5	4	3a	3b	35 (**1**) 33 (**2,3**)	36 (**1**) 34 (**2,3**)	37 (**1**) 35 (**2,3**)	10 (**1**,**2**) 8 (**3**)	11 (**1**,**2**) 9 (**3**)	12 (**1**,**2**) 10 (**3**)	15 (**1**,**2**) 13 (**3**)	16 (**1**,**2**) 14 (**3**)	19 (**1**,**2**) 17 (**3**)	20 (**1**,**2**) 18 (**3**)	21 (**1**,**2**) 19 (**3**)
δ_S	1.650	5.300	2.588	2.568	6.721	4.866	1.280	1.580	5.008	3.947	3.781	3.781	3.947	5.008	1.580
δ_R	1.610	5.352	2.669	2.589	6.960	4.918	1.310	1.490	5.018	3.992	3.932	3.932	3.992	5.018	1.490
$\Delta\delta_{S-R}$	+0.04	*R*	−0.071	−0.021	−0.239	−0.052	−0.030	+0.09	*R*	−0.045	−0.151	−0.151	−0.045	*R*	−0.09

TMSi derivative (**4b**) (Figure 5). The adjacent bis-THF ring moiety was determined to be located at C-13−C-22, while the third OH group was positioned at C-10. HREIMS identified the peak at *m*/*z* 427.2687 in **4b** as $C_{22}H_{43}O_4Si_2$ (calcd. 427.2700), and this important fragment confirmed the location of the THF ring moiety.

The relative configuration across the THF ring system of **4** was, again, determined as *threo*/*trans*/*threo*/*trans*/*threo*. To determine the relative stereochemistry at C-10/C-13, the formaldehyde acetal derivative (**4c**) was prepared.[13] The CIMS and EIMS fragmentations of **4c** confirmed that the formal acetal had formed between the two OH groups at C-10 and C-13. The acetal protons in **4c** were presented as a pair of doublets at δ 5.15 and 4.59 (J = 7.5 Hz) in the ^{1}H-NMR spectrum, indicating that the newly formed acetal ring possessed

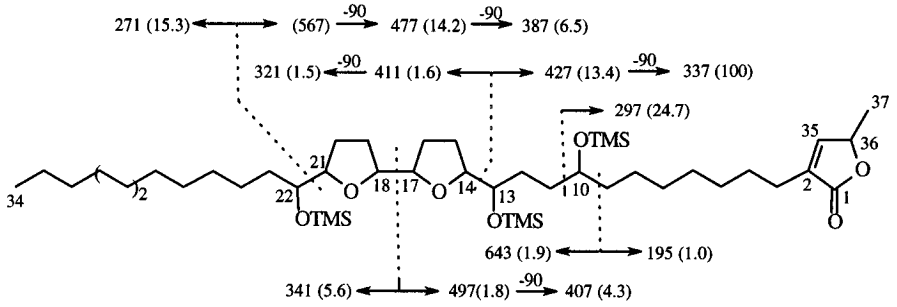

Figure 5. Diagnostic mass fragmentation ions of **4b** (molecular mass = 838 amu) in *m/z*, with percent intensities in parentheses. Losses of *m/z* 90 indicate the loss of TMSiOH neutrals.

Table 6. ^{1}H-NMR (500 MHz, $CDCl_3$) Data for MTPA Derivatives of **4c**

H no.	23	22	21	20a	20b	18	17	14
δ_S	1.62	5.02	4.05	1.93	1.51	3.83	3.92	3.95
δ_R	1.50	5.05	4.05	2.04	1.62	3.93	3.97	3.98
$\Delta\delta_{S-R}$	+0.12	*R*	0	−0.11	−0.11	−0.10	−0.05	−0.03

the *cis*- relative configuration, [13] and, thus, either an *S*/*S* or an *R*/*R* absolute configuration between C-10 and C-13 was revealed.

The absolute configuration of C-22 in **4c** was determined as *R*, again, by using advanced Mosher ester methodology (Table 6).[10] It then followed that those chiral centers at C-10, C-13, C-14, C-17, C-18, C-21, and C-22 were all *R* considering their relative stereochemistries. The absolute stereochemistry at C-36 was determined as *S* by observing a negative Cotton effect at 236 nm in the CD experiment, which was also observed for the model compound squamocin.[14,15] Thus, the structure of compound **4** was elucidated as illustrated and named longimicin D.

Longimicin D (**4**) is a structural isomer of asimicin, as well as a structural isomer of asimin.[16] Asimicin and asimin both have the THF ring moiety located at C-15−C-24, but asimicin has a 4-OH group while asimin has a 10-OH group. Longimicin D (**4**), like asimin, has a 10-OH group, but the THF ring moiety is located at C-13−C-22, shifted by two carbon units toward the terminal γ-lactone ring compared with asimicin and asimin.

Until now, 12 asimicin type acetogenins have been reported. The ring systems are all located at C13−C-22 for the C35 compounds and at C-15−C-24 for all the C37 compounds. Longimicin A−D (**1**−**4**) are the first examples among this type of acetogenins in which the THF ring systems are located at positions other than these two.

Bioactivities and SAR's. Biological activities of **1**−**4**, asimicin, asimin, and parviflorin are summarized in Table 7.[17] The four novel compounds (**1**−**4**) are all active in the BST[8,9] and in the yellow fever mosquito larvae assay;[18] these are two convenient bench-top bioassays routinely performed in our lab to discover new cytotoxic and pesticidal compounds. Compounds **1**−**4** also showed significant cytotoxicities against all six human tumor cell lines in our 7-day MTT human solid tumor cytotoxicity tests. Longimicin D (**4**) is generally more bioactive than **1**−**3**, whose cytotoxicities are still quite comparable to those of adriamycin, the positive control in the same run. Longimicin D (**4**) also showed some selectivity against the pancreatic carcinoma (PaCa-2)[19] cell line, exhibiting 3.5×10^5 times the potency of adriamycin.

Compared with the bioactivities of the known asimicin type acetogenins, **1**−**4** generally showed lower potencies than most of the known compounds. Therefore, it can be suggested that the position of the adjacent bis-THF ring system plays an important role in determining the relative activities of the asimicin type of acetogenins. To explore futher this speculation, the published bioactivities of the 12 known asimicin type compounds were compared. Compounds with the THF ring systems positioned at C-15−C-24 were generally much more active than those with the systems at C-13−C-22. Asimicin, asimin, asiminecin, and asiminocin, whose ring systems are located at C-15−C-24, are among the most potent bioactive acetogenins ever found.[16] However, the compounds with the rings at C-13−C-22 sometimes showed better selectivities against certain tumor cell lines. Parviflorin,[12] for example, showed notable selectivity against the lung cancer cell line (A-549)[20] with an ED_{50} value as low as $<10^{-12}$ μg/mL, while it was only moderately active against the human breast carcinoma (MCF-7)[21] and human colon adenocarcinoma (HT-29)[22] cell lines. Then we compared the cytotoxicities of the following structural isomers: asimicin[4,15] with longimicin A (**1**), asimin[15] with longimi-

Table 7. Bioactivity Data for Asimicin, Asimin, Parviflorin, Compounds **1**−**4**, and Adriamycin as the Positive Control Standard

	LC_{50} (μg/mL)		cytotoxicities: ED_{50} (μg/mL) against human tumor cell lines					
compound	BST[a]	YFM[b]	A-549[c]	MCF-7[d]	HT-29[e]	A-498[f]	PC-3[g]	PaCa-2[h]
asimicin[i]	2.6×10^{-2}	3.04	8.43×10^{-3}	8.52×10^{-1}	$<10^{-12}$	NT	NT	NT
asimin[i]	4.6×10^{-3}	NT	7.99×10^{-9}	9.57×10^{-9}	$<10^{-12}$	NT	NT	NT
parviflorin[j]	8.8×10^{-2}	NT	$<10^{-12}$	1.72	5.49×10^{-1}	NT	NT	NT
1	18.7	141	2.95×10^{-1}	8.89×10^{-1}	5.25×10^{-1}	5.44×10^{-1}	7.01×10^{-2}	1.73×10^{-2}
2	7.34	30.4	1.43×10^{-1}	1.54×10^{-2}	3.32×10^{-3}	6.40×10^{-2}	2.20	7.92×10^{-2}
3	9.42	75.7	4.55×10^{-1}	8.80×10^{-2}	1.00	1.27×10^{-1}	2.96	1.09
4	4.58	8.29	4.93×10^{-4}	2.15×10^{-1}	1.16×10^{-2}	3.53×10^{-2}	2.42×10^{-4}	1.69×10^{-7}
adriamycin	2.6×10^{-1}	NT	2.62×10^{-2}	1.94×10^{-1}	4.94×10^{-2}	6.63×10^{-2}	2.87×10^{-1}	3.40×10^{-2}

[a] Brine shrimp lethality test.[8,9] [b] Yellow fever mosquito larvae assay.[17] [c] Human lung carcinoma.[19] [d] Human breast carcinoma.[20] [e] Human colon adenocarcinoma.[21] [f] Human kidney carcinoma.[20] [g] Human prostate adenocarcinoma.[25] [h] Human pancreatic carcinoma.[18] [i] Data from Zhao *et al.*[16] [j] Data from Rantnayake *et al.*[12]

cin D (**4**), and parviflorin[12] with longimicins B (**2**) and C (**3**). The only differences between the isomers within each group was the position of the ring system. Longimicin A (**1**), with the ring system beginning at C-11, lost both potency and selectivity compared with asimicin. Longimicins B (**2**) and C (**3**), with the ring systems beginning at C-11 and C-9, respectively, showed neither significant cytotoxicity nor selectivity compared with parviflorin. Longimicin D (**4**), with the ring beginning at C-13, was less active than asimin; however, it showed selectivity against the pancreatic cancer cell line (PaCa-2).[19]

From the observations above, a sequence for the cytotoxicities of asimicin type acetogenins can be concluded as C-15−C-22 > C-13−C-20 > C-11−C-20 ≈ C-9−C-18. The optimal position for the THF ring system seems to be at C-15−C-24. When the ring systems shift to C-13−C-22, the compounds are less cytotoxic, but they sometimes show noteworthy selectivity.

From the published data, similar structure−activity relationships also can be observed with the bullatacin type Annonaceous acetogenins. Bullatacin[10,23] is the C-24 epimer of asimicin. Bullatacin, with the ring system at C-15−C-24, is highly potent against several human tumor cell lines. Squamotacin (C-37)[24] and molvizarin (C-35),[25] with the ring systems at C-13−C-22, are generally less active than bullatacin, but they both show significant selectivity against the human prostate tumor cell line (PC-3).[26]

The annonaceous acetogenins exert their effects, at least in part, through inhibition of oxygen uptake in mitochondrial electron transport systems at complex I.[27,28] In the rat liver mitochondrial assay, asimicin gave IC_{50} = 32 nM/mg of protein (rotenone used in the same run as a positive standard gave IC_{50} = 17 nM/mg of protein).[28] The acetogenins can also inhibit the NADH oxidase that is prevalent in the plasma membranes of tumor, but not normal, cells;[29] the resulting depletion of intracellular ATP levels induces *in vivo* antitumor effects, likely terminated by programmed cell death (apoptosis),[30] and especially suggests potential synergistic effects with other chemotherapeutic agents in the treatment of ATP dependent multidrug resistance.[31]

Experimental Section

Instrumentation. Melting points were determined on a Mettler FP5 hot-stage apparatus and are uncorrected. The optical rotations were determined on a Perkin-Elmer 241 polarimeter. UV spectra were taken in MeOH on a Beckman DU-7 spectrophotometer. IR spectra were obtained using NaCl plates on a Perkin-Elmer 1600 FTIR spectrophotometer. Low-resolution MS were recorded on a Finnigan 4000 mass spectrometer. The exact masses were determined on a Kratos 50 mass spectrometer through peak matching. ^{1}H- and ^{13}C-NMR spectra were recorded on a Varian VXR-500S spectrometer, using the Varian software systems. HPLC was carried out with Rainin HPLC instruments using the Dynamax software system and a Si gel column (250 × 21 mm, 8 μm, 60 Å) or a C-18 column (250 × 21 mm, 8 μm, 60 Å) equipped with a Rainin UV-1 detector set at 220 nm.

Derivatizations. (A) Preparation of Tri-TMSi Derivatives. Approximately 10−50 μg of pure acetogenins was placed in a 100 μL conical reaction vial and dried in a vacuum desiccator over P_2O_5 for 24 h. The sample was treated with 2 μL of pyridine and 20 μL of *N*,*O*-bis(trimethylsilyl)acetamide (BSA) (Pierce Chemical Co.) and heated at 70 °C for 30 min to yield the respective tri-TMSi derivatives (**1b**, **2b**, **3b**, and **4b**). The derivatives were directly transfered to a microvial for the EIMS measurements. The EIMS measurements were carried out at a resolution of 1500, scanning mass 900−100 at 30 s/decade.

(B) Preparation of Per-*S*- and Per-*R*-Mosher Esters. 0.5 mg of purified acetogenin was dissolved in 0.5 mL of CH_2Cl_2, and sequentially, 0.2 mL of pyridine, 0.2 mg of 4-(dimethylamino)pyridine, and 25 mg of (*R*)-(−)-α-methoxy-α-(trifloromethyl)phenylacetyl chloride (Aldrich) were added. The mixture was left at room temperature for 4 h and purified over a microcolumn (0.6 × 6 cm) of Si gel eluted with 2 mL of CH_2Cl_2; the eluate was washed with 1% $NaHCO_3$ (5 mL) and H_2O (5 mL × 2) and dried *in vacuo* to give the *S*-Mosher esters. Use of (*S*)-(+)-α-methoxy-α-(trifloromethyl)phenylacetyl chloride (Aldrich) gave the *R*-Mosher ester derivatives of acetogenins.

(C) Preparation of Acetate Derivatives. Pure acetogenin (1−2 mg) was dissolved in 0.5−1.0 mL of pyridine; 1 mL of anhydrous Ac_2O was added, and the mixture was set at room temperature for 4−8 h. The mixture was then partitioned between H_2O and CH_2Cl_2, and the organic layer was concentrated *in vacuo* to afford the pure acetate derivatives.

(D) Preparation of Intramolecular Formal Acetal Derivative 4c. A mixture of DMSO and TMSCl (molar ratio 1.2:1) was mixed in 2 mL of benzene and placed in a refrigerator without stirring for 2 h to allow the formation of white crystals. The benzene was decanted, and the crystals were washed twice with CH_2Cl_2. A large excess of the crystals was added to 0.5 mL of a $CHCl_3$ solution containing 16 mg of **4** at room temperature. After the mixture was heated to 65 °C for 1 min, the reaction was quenched with H_2O. After workup by extractions with 5% aqueous $NaHCO_3$, the reaction mixture was purified by normal phase HPLC to give 7.2 mg of **4c**.

Plant Material and Bioassays. The leaves and twigs of *A. longifolia* K. were collected in Georgia in September 1993 under the auspices of one of us (P.R.E.), Curator of the Herbarium, University of Georgia, where voucher specimens are maintained. The brine shrimp lethality test (BST) was performed as modified.[8,9] The yellow fever mosquito larvae assay was modified from the previously described procedure.[18] The cytotoxicity tests against A-549 (human lung carcinoma),[20] MCF-7 (human breast carcinoma),[21] HT-29 (human colon adenocarcinoma),[22] A-498 (human kidney carcinoma),[21] PC-3 (human prostate adenocarcinoma),[26] and PaCa-2 (human pancreatic carcinoma)[19] cells were performed in the Purdue Cell Culture Laboratory, Purdue Cancer Center, using standard protocols in 7-day assays with MTT and adriamycin as a positive standard control.

Extraction and Isolation. The residue of the 95% EtOH crude extract of 4 kg of the leaves and twigs was partitioned between H_2O and CH_2Cl_2 to give an H_2O layer and a CH_2Cl_2 layer. The residue of the CH_2Cl_2 layer was partitioned between hexane and 10% H_2O in MeOH to give an aqueous MeOH layer and a hexane layer. The MeOH residue (141 g), which was the most active fraction in the BST (LC_{50} 17.26 μg/mL), was repeatedly chromatographed over Si gel columns and chromatotron separations, directed by BST activity, using gradients of hexane/$CHCl_3$/MeOH and hexane/acetone, and finally purified by HPLC [Si gel column (8 μm, 60 Å), 10% MeOH/THF (9:1) in hexane; C-18 column (8 μm, 60 Å), 80% acetonitrile in H_2O] to give the four new acetogenins (**1**−**4**).

Longimicin A (1): colorless wax (10 mg); $[\alpha]_D$ +14 (EtOH, 1 mg/mL); UV λ_{max}^{MeOH} 208 nm; IR ν_{max}^{film} (cm^{-1}) 3400 (OH), 2925, 2855, 1750, 1457, 1318, 1200, 1069, 954, 870; HRFABMS (glycerol) *m*/*z* 623.4880 ([MH^+], found) (623.4887 calcd for $C_{37}H_{66}O_7$); EIMS (tri-TMSi derivative) see Figure 2; HREIMS (tri-TMSi derivative) *m*/*z* 399.2379 (found) (399.2387 calcd for $C_{20}H_{39}O_4Si_2$); ^{1}H-NMR and ^{13}C-NMR, see Table 1.

Longimicin B (2): colorless wax (7 mg); $[\alpha]_D$ +13 (EtOH, 1 mg/mL); UV λ_{max}^{MeOH} 208 nm; IR ν_{max}^{film} (cm^{-1}) 3438, 2925, 2855, 1752, 1457, 1318, 1200, 1069, 954, 870; HRFABMS (glycerol) *m*/*z* 595.4718 ([MH^+], found) (595.4754 calcd for $C_{35}H_{62}O_7$); EIMS (tri-TMSi derivative) see Figure 3; HREIMS (tri-TMSi derivative) *m*/*z* 399.2383 (found) (399.2387 calcd for

$C_{20}H_{39}O_4Si_2$), *m/z* 271.2454 (found) (271.2457 calcd for $C_{16}H_{35}OSi$); ^{1}H-NMR and ^{13}C-NMR, see Table 2.

Longimicin C (3): colorless wax (10 mg); $[\alpha]_D$ +14 (EtOH, 1 mg/mL); UV λ_{max}^{MeOH} 208 nm; IR ν_{max}^{film} (cm^{-1}) 3436, 2925, 2855, 1752, 1457, 1318, 1200, 1069, 954, 870; HRFABMS (glycerol) *m/z* 623.4880 ([MH^+], found) (623.4887 calcd for $C_{37}H_{66}O_7$); EIMS (tri-TMSi derivative) see Figure 4; HREIMS (tri-TMSi derivative) *m/z* 371.2074 (found) (371.2078 calcd for $C_{18}H_{35}O_4Si_2$), m/z 511.2911 (found) (511.2900 calcd for $C_{26}H_{47}O_6Si_2$); ^{1}H-NMR and ^{13}C-NMR, see Table 3.

Longimicin D (4): colorless wax (20 mg); $[\alpha]_D$ +14 (EtOH, 1 mg/mL); UV λ_{max}^{MeOH} 208 nm; IR ν_{max}^{film} (cm^{-1}) 3433, 2925, 2855, 1752, 1457, 1318, 1200, 1069, 954, 870; HRFABMS (glycerol) *m/z* 623.4880 ([MH^+], found) (623.4887 calcd for $C_{37}H_{66}O_7$); EIMS (tri-TMSi derivative), see Figure 5; HREIMS (tri-TMSi derivative) *m/z* 427.2687 (found) (427.2700 calcd for $C_{22}H_{43}O_4Si_2$); ^{1}H-NMR and ^{13}C-NMR, see Table 4.

Formal Acetal Derivative of Longimicin D (4c): colorless wax (7.2 mg); CIMS (isobutane) *m/z* 635 $[MH]^+$, 617 $[MH - H_2O]^+$, 605 $[MH - HCOH]^+$, 587 $[MH - HCOH - H_2O]^+$; EIMS *m/z* 199, 269, 295, 365, 435. ^{1}H-NMR, see Table 4.

Acknowledgment. This investigation was supported by RO1 Grant No. CA 30909 from the National Cancer Institute. Thanks are due to the Purdue Cell Culture Laboratory, Purdue Cancer Center, for the cytotoxicity testing.

References

(1) Rupprecht, J. K.; Hui, Y. H.; McLaughlin, J. L. Annonaceous Acetogenins: A Review. *J. Nat. Prod*. **1990**, *53*, 237−278.

(2) Fang, X. P.; Rieser, R. J.; Gu, Z. M.; Zhao, G. X.; McLaughlin, J. L. Annonaceous Acetogenins: An Updated Review. *Phytochem. Anal.* **1993**, *4*, 27−67.

(3) Gu, Z. M.; Zhao, G. X.; Oberlies, N. H.; Zeng, L.; McLaughlin, J. L. Annonaceous Acetogenins: Potent Mitochondrial Inhibitors with Diverse Applications. In *Recent Advances in Phytochemistry*; Arnason, J. T., Mata, R., Romeo, J. T., Eds.; Plenum Press: New York, 1995; Vol. 29, pp 249−310.

(4) Rupprecht, J. K.; Chang, C. J.; Cassady, J. M.; McLaughlin, J. L.; Mikolajczak, K. L.; Weisleder, D. Asimicin, a New Cytotoxic and Pesticidal Acetogenin from the Pawpaw, *Asimina triloba* (Annonaceae). *Heterocycles* **1986**, *24*, 1197−1201.

(5) Hoye, T. R.; Zhuang, Z. P. Validation of the ^{1}H NMR Chemical Shift Method for Determination of Stereochemistry in the Bis-(tetrahydrofuranyl)Moiety of Uvaricin-related Acetogenins from Annonaceae: Rolliniastatin 1 (And Asimicin). *J. Org. Chem*. **1988**, *53*, 5578−5580.

(6) Born, L.; Lieb, F.; Lorentzen, J. P.; Moescher, H.; Nonfon, M.; Sollner, R.; Wendisch, D. The Relative Configuration of Acetogenins Isolated from *Annona aquamosa*: Annonin I (squamocin) and Annonin VI. *Planta Med*. **1990**, *56*, 312−316.

(7) Alkofahi, A.; Rupprecht, J. K.; Anderson, J. E.; McLaughlin, J. L.; Mikolajczak, K. L.; Scott, B. A. Search for New Pesticides from Higher Plants. In *Insecticides of Plant Origin*; Arnason, J. T., Philogene, B. J. R., Morand, P., Eds.; ACS Symposium Series 2 No. 387; American Chemical Society: Washington, DC, 1989; pp 25−43.

(8) Meyer, B. N.; Ferrigni, N. R.; Putnam, J. E.; Jacobson, L. B.; Nichols, D. E.; McLaughlin, J. L. Brine Shrimp: A Convenient General Bioassay for Active Plant Constituents. *Planta Med*. **1982**, *45*, 31−34.

(9) McLaughlin, J. L. Crown Gall Tumors on Potato Discs and Brine Shrimp Lethality: Two Simple Bioassays for Higher Plant Screening and Fractionation. In *Methods in Plant Biochemistry*; Hostettmann, K., Ed.; Academic Press: New York, 1991; Vol. 6, pp 1−32.

(10) Rieser, M. J.; Hui, Y. H.; Rupprecht, J. K.; Kozlowski, J. F.; Wood, K. V.; McLaughlin, J. L.; Hanson, P. R.; Zhuang, Z.; Hoye, T. R. Determination of Absolute Configuration of Stereogenic Carbinol Centers in Annonaceous Acetogenins by ^{1}H- and ^{19}F-NMR Analysis of Mosher Ester Derivatives. *J. Am. Chem. Soc*. **1992**, *114*, 10203−10213.

(11) Hoye, T. R.; Hanson, P. R.; Hasenwinkel, L. E.; Ramirez, E. A.; Zhuang, Z. P. Stereostructural Studies on the 4-Hydroxylated Annonaceous Acetogenins: A Novel Use of Mosher Ester Data for Determining *Relative* Configuration [Between C(4) and C(36)]. *Tetrahedron Lett*. **1994**, *35*, 8529−8532.

(12) Ratnayake, S.; Gu, Z. M.; Miesbauer, L. R.; Smith, D. L.; Wood, K. V.; Evert, D. R.; McLaughlin, J. L. Parvifloracin and Parviflorin: Cytotoxic Bistetrahydrofuran Acetogenins with 35 Carbons from *Asimina parviflora* (Annonaceae). *Can. J. Chem*. **1994**, *72*, 287−293.

(13) Gu, Z. M.; Zeng, L.; Fang, X.-P.; Colman-Saizarbitoria, T.; Huo, M.; McLaughlin, J. L. Determining Absolute Configurations of Stereocenters in Annonaceous Acetogenins through Formaldehyde Acetal Derivatives and Mosher Ester Methodology. *J. Org. Chem*. **1994**, *59*, 5162−5172.

(14) Sahai, M.; Singh, S.; Singh, M.; Gupta, Y. K.; Akashi, S.; Yuji, R.; Hirayama, K.; Asaki, H.; Araya, H.; Hara, N.; Eguchi, T.; Kakinama, K.; Fujimoto, Y. Annonaceous Acetogenins from the Seeds of *Annona squamosa*: Adjacent Bis-tetrahydrofuranic Acetogenins. *Chem. Pharm. Bull*. **1994**, *42*, 1163−1174.

(15) Zhao, G. X.; Chao, J. F.; Zeng, L.; McLaughlin, J. L. The Absolute Configuration of Adjacent Bis-THF Acetogenins and Asiminocin, A Novel Highly Potent Asimicin Isomer from *Asimina triloba*. *Bioorg. Med. Chem.*, in press.

(16) Zhao, G. X.; Miesbauer, L. R.; Smith, D. L.; McLaughlin, J. L. Asimin, Asiminacin, and Asiminecin: Novel Highly Cytotoxic Asimicin Isomers from *Asimina triloba*. *J. Med. Chem*. **1994**, *37*, 1971−1976.

(17) In our 7-day MTT human tumor cytotoxicity test, the samples are serially diluted, and each concentration is tested in duplicate. The average values for each concentration are used to calculate an ED_{50} value. Adriamycin is used as a positive control in every experiment. Although the cell culture data of the seven compounds are obtained in three different runs, the bioactivities of adriamycin against each cell line in the three runs differs by less than 2 orders of magnitude, demonstrating the reliability of the bioactivity data.

(18) Instructions for Determining the Susceptibility or Resistence of Adult Mosquitoes to Organochlorine Insecticides. *WHO Tech. Rep. Ser*. **1970**, No. 443, pp 47−55.

(19) Yunis, A. A.; Arimura, G. K.; Russian, D. Human Pancreatic Carcinoma (MIA PaCa-2) in Continuing Culture: Sensitivity to Asparaginase. *Int. J. Cancer* **1977**, *19*, 128−135.

(20) Giard, D. J.; Aronson, S. A.; Todaro, G. J.; Arnstein, P.; Kersey, H. J.; Dosik, H.; and Parks, W. P. In Vitro Cultivation of Human Tumors: Establishment of Cell Lines Derived from a Series of Solid Tumors. *J. Natl. Cancer Inst*. **1973**, *51*, 1417−1423.

(21) Soule, H. D.; Vazquez, J.; Long, A.; Albert, S.; Brennan, M. A Human Cell Line from a Pleural Effusion Derived from A Breast Carcinoma. *J. Natl. Cancer Inst*. **1973**, *51*, 1409−1413.

(22) Fogh, J.; Trempe, G. New Human Tumor Cell Lines. In *Human Tumor Cell Lines In Vitro*; Fogh, J., Ed.; Plenum Press: New York, 1975; pp 115−159.

(23) Hui, Y. H.; Rupprecht, J. K.; Anderson, J. E.; Liu, Y. M.; Smith, D. L.; Chang, C. J.; McLaughlin, J. L. Bullatacin and Bullatacinone: Two Highly Potent Bioactive Acetogenins from *Annona bullata*. *J. Nat. Prod*. **1989**, *52*, 463−477.

(24) Hopp, D. C.; Zeng, L.; Gu, Z. M.; McLaughlin, J. L. Squamotacin: An Annonaceous Acetogenin with Cytotoxic Selectivity for the Human Prostate Tumor Cell Line (PC-3). *J. Nat. Prod*. **1996**, *59*, 97−99.

(25) Cortes, D.; Myint, S. H.; Hocquemiller, R. Molvizarin and Motrilin: Two Novel Cytotoxic Bis-tetrahydrofuranic γ-lactone Acetogenins from *Annona cherimolia*. *Tetrahedron* **1991**, *47*, 8195−8202.

(26) Kaighn, M. E.; Narayan, K. S.; Ohinuki, Y.; Lechner, J. F.; Jones, L. W. Establishment and Characterization of a Human Prostatic Carcinoma Cell Line (PC-3). *Invest. Urol*. **1979**, *17*, 16−23.

(27) Ahammadsahib, K. I.; Hollingworth, R. M.; McGovern, J. P.; Hui, Y. H.; McLaughlin, J. L. Mode of Action of Bullatacin: A Potent Antitumor and Pesticidal Annonaceous Acetogenin. *Life Sci*. **1993**, *53*, 1113−1120.

(28) Landolt, J. L.; Ahammadsahib, K. I.; Hollingworth, R. M.; Barr, R.; Crane, F. L.; Burck, N. L.; McCabe, G. P.; McLaughlin, J. L. Determination of Structure-Activity Relationships of Annonaceous Acetogenins by Inhibition of Oxygen Uptake in Rat Liver Mitochondria. *Chem. Biol. Interact*. **1995**, *98*, 1−13.

(29) Morré, D. J.; de Cabo, R.; Farley, C.; Oberlies, N. H.; McLaughlin, J. L. Mode of Action of Bullatacin, a Potent Antitumor Acetogenin: Inhibition of NADH Oxidase Activity of HELA and HL-60, but not Liver, Plasma Membranes. *Life Sci*. **1995**, *56*, 343−350.

(30) Wolvetang, E. J.; Johnson, K. L.; Krauer, K.; Ralph, S. J.; Linnane, A. W. Mitochondrial Respiratory Chain Inhibitors Induce Apoptosis. *FEBS Lett*. **1994**, *339*, 40−44.

(31) Oberlies, N. H.; Jones, J. L.; Corbett, T. H.; Fotopoulos, S. S.; McLaughlin, J. L. Tumor Cell Growth Inhibition by Several Annonaceous Acetogenins in an in vitro Disk Diffusion Assay. *Cancer Lett*. **1995**, *96*, 55−62.

JM9600510